ResearchGate

See discussions, stats, and author profiles for this publication at: https://www.researchgate.net/publication/243658053

Hydrogen evolution at a platinum-modified indium phosphide photoelectrode: improvement of current-voltage characteristics by hydrogen chloride etching

ARTICLE *in* THE JOURNAL OF PHYSICAL CHEMISTRY · JANUARY 1991

Impact Factor: 2.78 · DOI: 10.1021/j100155a062

CITATIONS
26

READS
12

4 AUTHORS, INCLUDING:

Hikaru Kobayashi
Osaka University, Faculty of Engineering Scie…

201 PUBLICATIONS **2,780** CITATIONS

SEE PROFILE

Available from: Hikaru Kobayashi
Retrieved on: 25 January 2016

fusional and therefore more sensitive to changes in intermolecular interactions.

Using bulk theories of relaxation for surface-associated CD_3CN, we have shown that the rotational motion is anisotropic, independent of the amount of sorbed CD_3CN and the rotational diffusion model (eq 2). We feel that relaxation measurements of this nature are valuable for probing the surface character of the materials studied here and elsewhere.

Acknowledgment. This work was supported by NSF Grant CHE-8719266. We thank Professor Joel Harris for his helpful discussions and Professor John Dorsey for supplying the partially deactivated silicas.

Registry No. MeCN, 75-05-8.

Silicon–Nonaqueous Solution Interface Studied by Capacitance–Voltage and Conductance–Voltage Techniques

Hikaru Kobayashi,* Nobuteru Takeda, Hiroshi Sugahara, and Hiroshi Tsubomura*

Laboratory for Chemical Energy Conversion and Department of Chemistry, Faculty of Engineering Science, Osaka University, Toyonaka, Osaka, 560 Japan *(Received: April 6, 1990; In Final Form: August 9, 1990)*

The capacitance–voltage and conductance–voltage techniques are applied to the study of the silicon–acetonitrile and silicon–methanol interfaces. The flat-band potential of the silicon electrode in these solutions shows an irreversible anodic shift during successive sweeps of the electrode potential, the amount of the shift depending on the electrolytes, the solvents, and the potential sweep regions. XPS spectra show that a silicon oxide layer is formed after the potential sweeps, and cations of the electrolytes are included in the oxide layer. This cation inclusion causes a potential drop across this layer, enhancing the barrier height in the silicon. The capacitance and conductance peaks observed for the silicon electrodes immersed in these solutions are attributable more probably to minority carriers in the surface region than surface states. The time constant for the conductance peak is longer than 3×10^{-2} s in the dark, while it decreases to $\sim 2 \times 10^{-4}$ s under illumination due to an increase in the minority carrier generation rate in the silicon. In the presence of the redox couple in the solution, the minority carrier quasi-Fermi level at the surface coincides with the redox level in the small bias region, and the linear Mott–Schottky plot arises.

Introduction

The properties of semiconductor–solution interfaces are important not only from the scientific point of view but also for the application of photoelectrochemical (PEC) cells. In the present study, the capacitance–voltage (C–V) and conductance–voltage (G–V) techniques are applied to elucidate the characteristics of silicon–acetonitrile (or methanol) interfaces.

The flat-band potential (abbreviated E_{FB} hereafter) of a semiconductor can be obtained from the C–V measurements. Formation of a high barrier is necessary to achieve high-energy conversion efficiency of solar cells, and artificial control of E_{FB} may help to attain it. The E_{FB} of a PEC cell is frequently shifted by the adsorption of solutes[1-3] and solvents,[4] which induces an electrical double layer. On the other hand, the shift of E_{FB} in metal–insulator–semiconductor (MIS) devices is caused mainly by the charge near the semiconductor–insulator interface[5-9] and is often proportional to the thickness of the insulating layer.[7-9] This shift is applied to MIS inversion layer solar cells[10-15] in which relatively thick oxide layers are formed. As the insulating layer becomes thinner, the amount of the shift of E_{FB} decreases, and consequently, the barrier height becomes low. In this paper, a procedure to include a large amount of ions into the silicon oxide layer of thickness below 30 Å is reported by which a large shift of E_{FB} can be achieved in such a thin insulating layer.

C–V and G–V measurements are used to obtain information on surface states present in MIS devices[16-20] as well as semiconductors immersed in electrolyte solutions.[4,21-24] Some workers observed peaks in the C–V curves for semiconductors in solutions and attributed them to the existence of surface states, although the state densities estimated from the peak intensity are much higher than those for conventional MIS devices. For the case of

(1) Minoura, H.; Tsuiki, M. *Electrochim. Acta* **1978**, *23*, 1377.
(2) Matsumura, M.; Hiramoto, M.; Iehara, T.; Tsubomura, H. *J. Phys. Chem.* **1984**, *88*, 248.
(3) Uchihara, T.; Matsumura, M.; Ono, J.; Tsubomura, H. *J. Phys. Chem.* **1990**, *94*, 415.
(4) Chazalviel, J.-N. *J. Electroanal. Chem.* **1987**, *233*, 37.
(5) Deal, B. E. *J. Electrochem. Soc.* **1967**, *114*, 226.
(6) Deal, B. E. *J. Electrochem. Soc.* **1974**, *121*, 198C.
(7) Hickmott, T. W. *J. Appl. Phys.* **1980**, *51*, 4269.
(8) Razouk, R. R.; Deal, B. E. *J. Electrochem. Soc.* **1982**, *129*, 806.
(9) Akinwande, A. I.; Plummer, J. D. *J. Electrochem. Soc.* **1987**, *134*, 2297.
(10) Salter, G. C.; Thomas, R. E. *Solid-State Electron.* **1977**, *20*, 95.
(11) Godfrey, R. B.; Green, M. A. *Appl. Phys. Lett.* **1979**, *34*, 790.
(12) Godfrey, R. B.; Green, M. A. *IEEE Trans. Electron Devices* **1980**, *27*, 737.
(13) Matsuura, H.; Fujii, H.; Takai, H.; Matsunami, H. *Jpn. J. Appl. Phys.* **1982**, *21*, 117.
(14) Hezel, R.; Schorner, R. *J. Appl. Phys.* **1981**, *52*, 3076.
(15) Hezel, R. *Solid-State Electron.* **1981**, *24*, 863.
(16) Nicollian, E. H.; Goetzberger, A. *Bell Syst. Tech. J.* **1967**, *46*, 1055.
(17) Grove, A. S.; Deal, B. E.; Snow, E. H.; Sah, C. T. *Solid-State Electron.* **1965**, *8*, 145.
(18) Kuhn, M. *Solid-State Electron.* **1970**, *13*, 873.
(19) Shewchun, J.; Green, M. A.; King, F. D. *Solid-State Electron.* **1974**, *17*, 563.
(20) Haddara, H. S.; El-Sayed, M. *Solid-State Electron.* **1988**, *31*, 1289.
(21) Madou, M. J.; Loo, B. H.; Frese, K. W.; Morrison, S. R. *Surf. Sci.* **1981**, *108*, 135.
(22) Nagasubramanian, G.; Wheeler, B. L.; Hope, G. A.; Bard, A. J. *J. Electrochem. Soc.* **1983**, *130*, 385.
(23) Nagasubramanian, G.; Wheeler, B. L.; Bard, A. J. *J. Electrochem. Soc.* **1983**, *130*, 1680.
(24) Rao, A. V.; Chazalviel, J.-N.; Ozanam, F. *J. Appl. Phys.* **1986**, *60*, 696.

0022-3654/91/2095-0813$02.50/0 © 1991 American Chemical Society

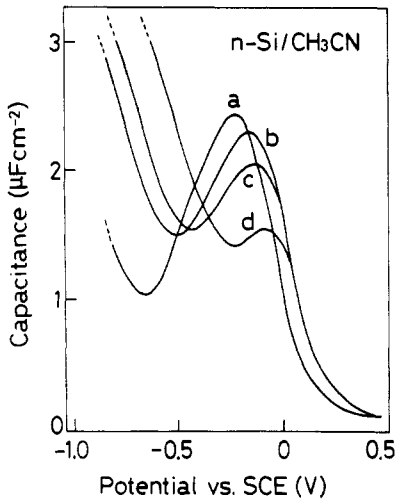

Figure 1. Change of the C–V curve for the n-Si electrode in a 1 M acetonitrile solution of $LiClO_4$ as the number of the potential sweep cycles is increased: (a) the first cycle, (b) the second cycle, (c) the third cycle, and (d) after stabilization of the C–V curve. The sweeping range is between −0.8 and 1.5 V vs SCE, and the presented curves are measured during the potential sweep from −0.8 to 0.5 V.

n-Si electrodes immersed in a methanol solution, capacitance peaks are also observed and attributed to surface states.[4] On the contrary, Lewis et al.[25] and we[26] have shown that high photovoltages can be obtained from these electrodes in methanol solutions. These results as well as our recent analysis of the ideality factor[27] indicate that the electron–hole recombination rate at the Si–methanol interface is negligibly small.

Experimental Section

The semiconductor electrodes were prepared from n-Si (phosphorus doped, 12 Ω cm unless otherwise noted) and p-Si (boron doped, 150 Ω cm) wafers. After washing with deionized water and boiled acetone, the Si wafers (10 × 10 mm^2) were put in a boiled H_2SO_4 + HNO_3 (1:1) solution followed by etching with a 25% HF solution. Then, a thin silicon oxide layer was formed in a boiled HNO_3, and the oxide layer was removed with an HF solution. Ohmic contact was made with In–Ga alloy, the Cu wire was attached to the rear surface for current collection, and then the electrode was encapsulated with epoxy resin. Immediately after etching the Si electrode with HF and washing it with acetonitrile or methanol, the C–V and G–V characteristics were measured in acetonitrile or methanol solutions. Silicon oxide layers were produced by immersing bare Si wafers in nitric acid kept at 363 K for 10 min.

The solvent used was reagent grade acetonitrile or methanol stored with molecular sieve. Solutions of 1 M $LiClO_4$ or $NaClO_4$ were used. For some experiments, 50 mM 1,1′-dimethylferrocene, $(Me)_2Fc$, and 5 mM of its oxidized product, $(Me)_2Fc^+$, were added in the solution as a redox couple. The C–V and G–V measurements were performed with a plain platinum (Pt) counter electrode and a saturated calomel reference electrode (SCE). When the solution contained a redox couple, a plain Pt was used as a reference electrode. In other words, the electrode potential was measured with respect to the redox level. The SCE was kept in a separate tube which contained a solution of the same composition as that of the main cell and connected to the cell with a liquid junction. The C–V and G–V measurements were made with an impedance analyzer (Hewlett-Packard, Model 4192A) and a potential sweeper at the frequency in the range between 5 and 10^4 Hz. The peak-to-peak amplitude of the ac signal was usually 5 mV and increased to 25 mV when the frequency was below 30 Hz. The potential sweep rate in the measurement of the shift in E_{FB} was 8 mV s^{-1}. The C–V measurements under illumination were carried out using a tungsten–halogen lamp with the light intensity at the sample position of 10 mW cm^{-2}. The temperature-dependent measurements of the C–V curve were performed by keeping the main cell in acetone containing dry ice.

The XPS spectra were measured with a Shimadzu ESCA 750 spectrometer.[28] The binding energies were corrected by using the C 1s peak of contaminant carbon as an energy standard (285 eV). The thickness of the silicon oxide layer was estimated from the intensity ratio of the Si 2p peak originating from the silicon oxide and that of bulk Si.

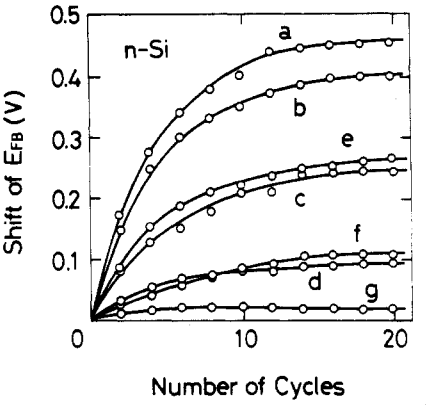

Figure 2. Shifts of E_{FB} of the n-Si electrode as a function of the number of the potential sweep cycles for the regions between: (a) −1.0 and 1.0 V in acetonitrile containing 1 M $LiClO_4$, (b) −1.0 and 0.5 V in the same solution as (a), (c) −1.0 and 0.25 V in the same solution as (a), (d) −1.0 and 0 V in the same solution as (a), (e) −1.0 and 1.0 V in acetonitrile containing $NaClO_4$, (f) −1.0 and 1.0 in methanol containing 1 M $LiClO_4$, and (g) −1.0 and 1.0 V for the 15-Å-thick SiO_2 covered n-Si in acetonitrile containing 1 M $LiClO_4$.

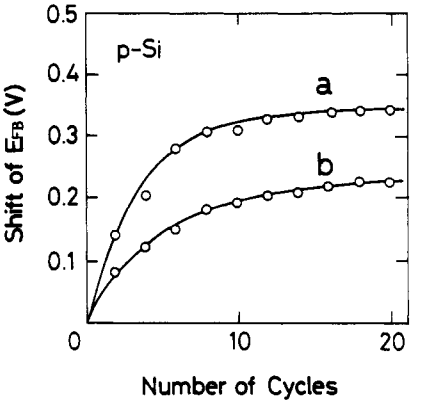

Figure 3. Shifts of E_{FB} of the p-Si electrodes immersed in a 1 M acetonitrile solution of $LiClO_4$ as a function of the number of the potential sweep cycles for the ranges between (a) −1.0 and 1.0 V and (b) −1.0 and 0.5 V.

Results

Figure 1 shows the change in the C–V curves for the n-Si electrode in a 1 M acetonitrile solution of $LiClO_4$ with the number of the potential sweep cycles, in the potential sweep range between −0.8 and 0.5 V vs SCE, although the potential was swept from −0.8 to 1.5 V during the measurements. As the potential sweep was repeated, the C–V curve was shifted to the anodic direction.

In Figure 2 are plotted the shifts of E_{FB}'s for the n-Si electrodes vs the number of the potential sweep cycles. E_{FB} always shifted in the anodic direction with the sweep cycles, and the amount of the shift depended on the electrolytes, the solvents, and the regions of the sweep. By expanding the potential sweep range, the shift became larger and irreversible; i.e., once the shift was caused, the

(25) Rosenbluth, M. L.; Lewis, N. S. *J. Am. Chem. Soc.* **1986**, *108*, 4689.
(26) Kobayashi, H.; Tsubomura, H. *J. Electroanal. Chem.* **1989**, *272*, 37.
(27) Kobayashi, H.; Chigami, A.; Takeda, N.; Tsubomura, H. *J. Electroanal. Chem.*, in press.
(28) Nakato, Y.; Yoshimura, M.; Hiramoto, M.; Tsumura, A.; Murahashi, T.; Tsubomura, H. *Bull Chem. Soc. Jpn.* **1984**, *57*, 355.

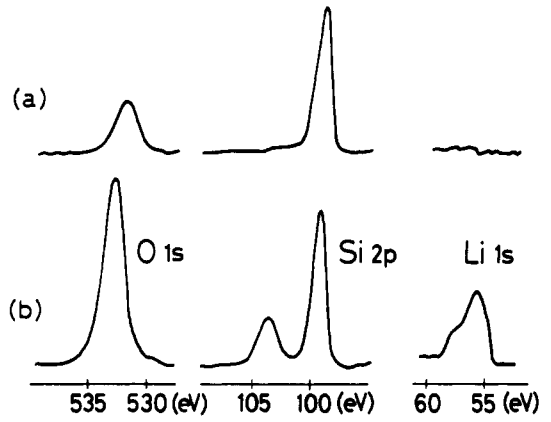

Figure 4. XPS spectra in the O 1s, Si 2p, and Li 1s regions of the n-Si electrode: (a) after keeping the electrode in a 1 M acetonitrile solution of $LiClO_4$ for 30 min without applying potential and (b) after 20 cycles of the potential sweep between −1.0 and 1.0 V vs SCE in the same solution.

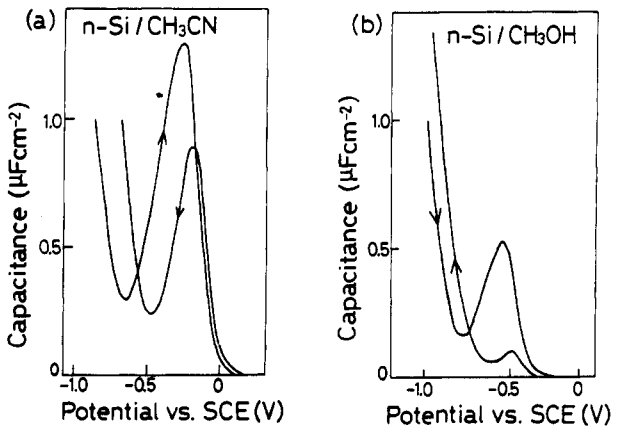

Figure 5. Capacitance–voltage curves measured at 293 K for the n-Si electrode: (a) in a 1 M acetonitrile solution of $LiClO_4$ and (b) in a 1 M methanol solution in $LiClO_4$.

amount was not reduced by contracting the potential sweep region. By use of $NaClO_4$ as an electrolyte, the amount of the shift became nearly one-half that of using $LiClO_4$ for the same sweep range. In methanol, the amount of the shift was about one-fourth of that in acetonitrile. In all cases, most of the shift occurred during the initial 10 cycles and the E_{FB} value was stabilized after 20 cycles. The largest shift of ~0.5 V occurred for the case of a Si electrode immersed in a 1 M acetonitrile solution of $LiClO_4$ after the potential sweep between −1.0 and 1.0 V vs SCE. For an n-Si electrode on which a 15-Å-thick SiO_2 layer was formed by the use of HNO_3, the shift of E_{FB} by the potential sweep was very small.

For the case of a p-Si electrode in 1 M acetonitrile solutions of $LiClO_4$, E_{FB} shifted in the positive direction with the sweep cycles as shown in Figure 3, similar to that for the n-Si electrode. By expanding the potential sweep range, the amount of the shift was increased.

Figure 4 shows the XPS spectra measured after immersing the n-Si electrode in a 1 M acetonitrile solution of $LiClO_4$. After 20 cycles of the potential sweep between −1.0 and 1.0 V vs SCE (corresponding to curve a in Figure 2), the intensity of the O 1s peak increased, the Li 1s peak appeared, the original Si 2p peak at 99.2 eV decreased in intensity, and a new Si 2p peak appeared at 103.8 eV. In the Li 1s region, the main peak and a shoulder appeared at 55.8 and 57.8 eV, respectively. By expanding the potential sweep range to the positive direction, the intensity of the O 1s and the shifted Si 2p peaks increased, indicating the formation of a thicker silicon oxide layer, and that of the Li 1s peak also increased.

Figure 5 shows the C–V curves for n-Si electrodes immersed in 1 M acetonitrile and methanol solutions of $LiClO_4$, measured

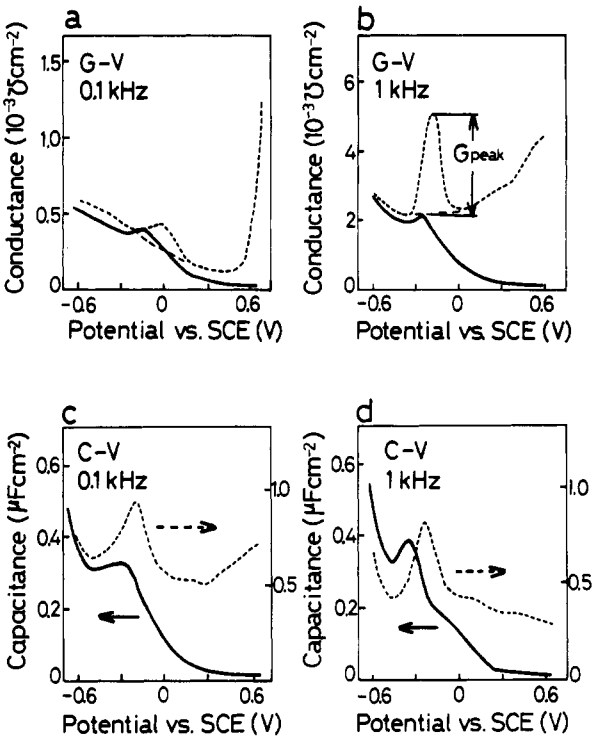

Figure 6. C–V and G–V curves for the n-Si electrode in a 1 M acetonitrile solution of $LiClO_4$: (a) G–V curve at 0.1 kHz, (b) G–V curve at 1 kHz, (c) C–V curve at 0.1 kHz, and (d) C–V curve at 1 kHz. The solid and dotted lines show the curves measured in the dark and under illumination, respectively. The conductance peak intensity, G_{peak}, is estimated by subtracting the background due to the faradaic resistance shown by the dashed line.

at 1 kHz. A peak and hysteresis were observed in both cases. The magnitude of hysteresis, defined here by the voltage difference between the positive-to-negative sweep and the reverse sweep in the region where the curves for both sweeps were almost parallel to each other, was found to depend on the potential sweep region. Hysteresis was not observed for the n-Si electrode in acetonitrile when the electrode potential was swept between −0.9 and −0.6 V vs SCE. By expanding the sweep region to the positive, the C–V curve for the positive-to-negative sweep was shifted in the positive direction. The magnitude of hysteresis for the potential sweeps between −0.9 and −0.35, −0.9 and 0, −0.9 and 0.25, −0.9 and 0.5, −0.9 and 0.75, and −0.9 and 1.0 V were respectively 30, 140, 200, 290, 310, and 360 mV. On the other hand, when the potential sweep region was expanded negative of −0.9 V, the C–V curve for the negative-to-positive sweep showed a cathodic shift. The magnitude of hysteresis for the potential sweeps between −0.6 and −1.15, −0.6 and −1.3, and −0.6 and −1.55 V were respectively 80, 110, and 160 mV. Similar hysteresis was observed for the Si electrodes in methanol. The C–V curves shown in Figure 5 agree with the results reported by others.[4,29]

Figure 6 shows the C–V and G–V curves for the n-Si electrodes immersed in a 1 M acetonitrile solution of $LiClO_4$, measured both in the dark (solid line) and under illumination (dotted line) at 0.1 and 1 kHz. A peak was present in each curve, and its intensity was increased by illumination. The measured conductance was divided into two parts as shown by the dashed line, i.e., the background due to the faradaic resistance related to majority carrier transport and the peak, G_{peak}. The peak position in the G–V curves showed fluctuation with ca. 0.2 V from time to time and from sample to sample, because of the change of the G–V curve with time, similar to the C–V curve as shown in Figure 1 and of the dependence on the conditions of the potential sweep. By repeated careful observation of the G–V curves, however, we concluded that the peak position was independent of the ac fre-

(29) Turner, J. A.; Manassen, J.; Nozik, A. J. *Appl. Phys. Lett.* **1980**, *37*, 488.

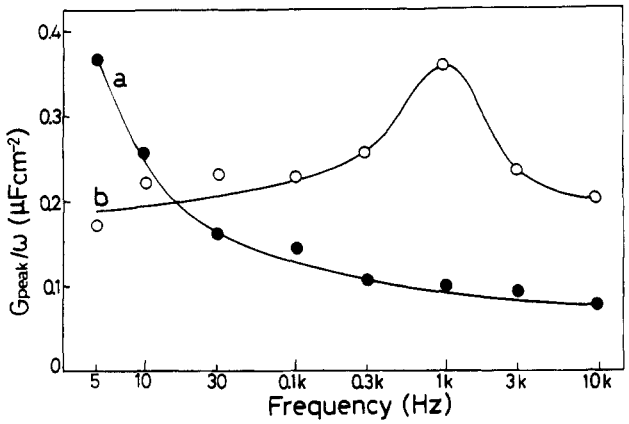

Figure 7. Plots of the conductance peak intensity, G_{peak}, divided by the angular frequency, ω, vs the frequency measured (a) in the dark and (b) under illumination.

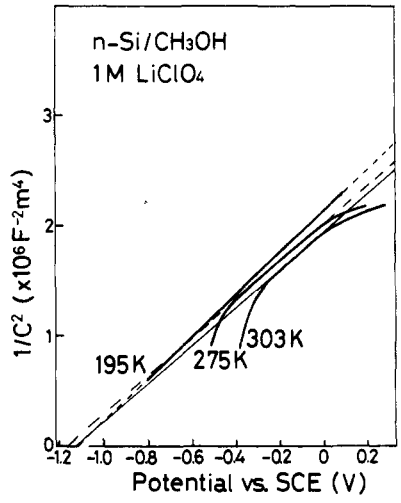

Figure 8. Mott-Schottky plots measured in the dark at 1 kHz for the n-Si electrode in a 1 M methanol solution of $LiClO_4$ kept at 303, 275, and 195 K. The resistivity of the Si electrode is 0.1 Ω cm.

quency and stayed at around −0.2 V vs SCE.

Figure 7 shows the plots of the conductance peak intensity, G_{peak}, at around −0.2 V divided by the angular frequency of the ac signal, ω, vs the frequency. The G_{peak}/ω measured in the dark decreased monotonically with the frequency, while the plot observed under illumination had a maximum at ~1 kHz.

Figure 8 shows the Mott-Schottky plots for the n-Si electrode immersed in a 1 M methanol solution of $LiClO_4$, measured at 1 kHz in the dark, the Si resistivity being 0.1 Ω cm in this case. The Mott-Schottky plot recorded at 195 K was linear in the voltage range between −0.8 and 0.1 V vs SCE. When the temperature was raised to 275 K, the plot deviated from the straight line in the region of potential less than −0.4 V. At 303 K, the linear portion of the plot was further reduced. The straight lines for the measurements at 275 and 303 K were drawn by assuming that they had the slopes the same as that for 195 K adjusted by taking account of the change in the ionization probability of the donor atoms at different temperatures.

Figure 9 shows the Mott-Schottky plot for the n-Si electrode immersed in a 1 M methanol solution of $LiClO_4$, measured at 1 kHz in the dark. The solution contained 50 mM $(Me)_2Fc$ and 5 mM $(Me)_2Fc^+$ as a redox couple, and the potential was measured with respect to the redox level. The plot was linear in the small bias region between −0.4 and 0.4 V. The intercept with the x axis of the straight line extrapolated, V_x, was 0.8 V. The corresponding barrier height is estimated via the following equation

$$\phi = V_x - kT/e_0 + \Delta_F \qquad (1)$$

where k is the Boltzmann constant, T is the temperature, e_0 is the elementary electric charge, and Δ_F is the potential difference between the Fermi level and the bottom of the conduction band in the bulk. Δ_F is estimated to be 0.28 V from the donor density of 3.5×10^{14} cm^{-3}, and hence ϕ is calculated to be 1.06 V from eq 1.

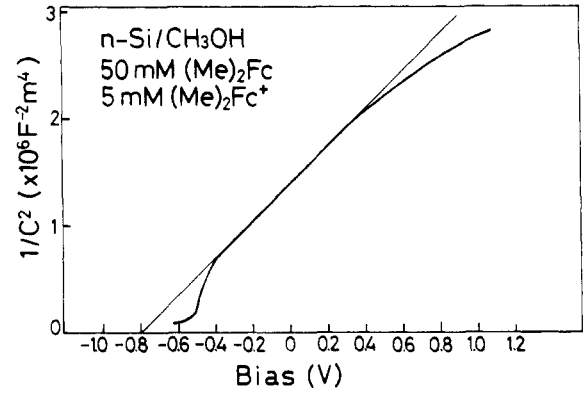

Figure 9. Mott-Schottky plot for the n-Si electrode in a 1 M methanol solution of $LiClO_4$ containing 50 mM $(CH_3)_2Fc$ and 5 mM $(CH_3)_2Fc^+$ as a redox couple, measured in the dark at 1 kHz.

Discussion

The Shift of C-V Curves. The shift of the C-V curves can be divided into two parts, i.e., a permanent shift and a reversible shift (hysteresis).

Both n- and p-Si electrodes show irreversible anodic shifts of E_{FB} with repeated potential sweep cycles. The amount of the anodic shift depends on the potential sweep region, and once it occurs, it persists even when the sweep range is reduced. In the XPS spectra of the electrode where 0.5 eV shift of E_{FB} is caused (curve a in Figure 2), a new Si 2p peak appears at 103.8 eV, in addition to the 99.2-eV peak due to the bulk Si. The energy difference between these peaks (4.6 eV) indicates that the 103.8-eV peak is due to SiO_2, i.e., a Si atom bound to four oxygen atoms.[30,31] By taking the escape depth of Si 2p photoelectrons to be 27 Å,[32] and the density of the Si oxide to be 2.2 g cm^{-3}, the thickness of the oxide layer is estimated to be 30 Å from the intensity ratio of the 103.8-eV peak to the 99.2-eV peak. After the potential sweep, a Li 1s peak appears at 55.8 eV with a shoulder at 57.8 eV. The peak is attributed to a Li atom bound to silicon or oxygen and the shoulder to free Li^+ ions. From the depth profile of the XPS spectra, it is found that these Li species are present in the SiO_2 layer. The former Li species is thought to form highly polarized bonds, such as Li^+–O^-, and it has no net effect on the potential since the dipole moments of these bonds point to random directions, and hence, it causes no shift of E_{FB}. On the other hand, free Li^+ ions shift the E_{FB} as discussed later. For the case where $NaClO_4$ is used as a supporting electrolyte instead of $LiClO_4$, the magnitude of the shift is reduced to one-half. The smaller shift for $NaClO_4$ indicates that the confinement of Na^+ ions is more difficult than Li^+ ions probably because Na^+ has a larger ionic radius (0.95 Å) than Li^+ (0.60 Å).

Figure 10 shows schematic illustrations of the charge distribution and potential diagrams for the Si/SiO_2/solution systems. For the dopant density of 3.5×10^{14} cm^{-3} corresponding to the Si resistivity of 12 Ω cm[33] and the band bending of 0.8 V, the potential drop across a 30-Å-thick SiO_2 layer caused by the depletion layer charge due to ionized donors is estimated to be 8.7 mV in the absence of ions in this layer, assuming that the dielectric constant of the SiO_2 layer is 3.8. Hence, it is negligibly small compared with the Si band bending. On the other hand, a substantial potential drop occurs across the SiO_2 layer in cases where

(30) Hollinger, G.; Himpsel, F. J. *J. Vac. Sci. Technol.* **1983**, *A1*, 640.
(31) Su, C. Y.; Skeath, P. R.; Lindau, I.; Spicer, W. *J. Vac. Sci. Technol.* **1981**, *18*, 843.
(32) Bechstedp, P.; Hubner, K. *Phys. Status Solidi* **1981**, *A67*, 517.
(33) Sze, S. M. *Physics of Semiconductor Devices*, 2nd ed.; John Wiley: New York, 1981; Chapter 1.

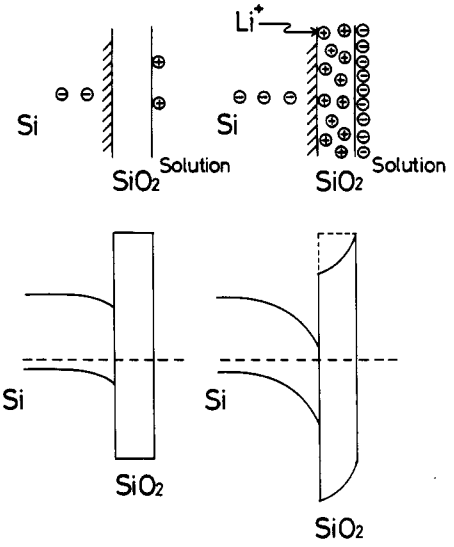

Figure 10. Potential diagrams for p-Si/SiO_2/solution system. In the absence of ions in the SiO_2 layer, the potential in this layer is almost flat in cases where the dopant density in the Si is below 10^{16} cm^{-3} (a), while a potential drop occurs across the SiO_2 layer in the presence of ions in this layer (b).

excess charges are present in the layer as illustrated in Figure 10b, which is given by

$$V_I = e_0 \int_0^d x N_I(x)\, dx/\epsilon_I \qquad (2)$$

where x is the distance from the SiO_2 outer surface, N_I is the charge density, d is the thickness of the SiO_2 layer, and ϵ_I is the permittivity of SiO_2. Accordingly, the Si band edges are moved down by V_I, while the Fermi level of the Si is aligned with the redox level. Therefore, in cases where positive ions are present in the SiO_2 layer, this shift of the band edges increases the barrier height for a p-Si electrode, while that for an n-Si electrode is reduced. Assuming that cations are uniformly distributed in the SiO_2 layer, the ion density, N_I, to cause a 0.5-V shift of E_{FB} is estimated to be 2×10^{19} cm^{-3} for $d = 30$ Å.

When an n-Si electrode covered with a 30-Å-thick oxide layer was prepared and the potential sweep was carried out for this electrode, E_{FB} was not changed. This indicates that the cations are brought into the SiO_2 layer while the oxide layer grows, but not after the formation of the oxide layer.

The amount of the shift of E_{FB} depends on the sweep range. By expanding the potential range to the positive direction, the oxide layer becomes thicker, and the amount of Li confined in this layer is increased. Both of these effects increase the amount of the shift.

The amount of the shift was smaller when methanol was used as a solvent. It is highly probable that this smaller shift in methanol arises from the larger amount of water contained in methanol than in acetonitrile. This is proved by the phenomenon that the shift of E_{FB} becomes much smaller for the Si electrode immersed in acetonitrile into which a few drops of water are introduced intentionally.

The magnitude of hysteresis depends on the extent of the potential sweep. For the n-Si electrode in acetonitrile, hysteresis is not observed by moving the electrode potential between −0.9 and −0.6 V vs SCE. By expanding the range toward the positive, the C–V curve for the positive-to-negative sweep is shifted to the positive. Hysteresis is caused by slow surface states localized either on surface Si atoms or adsorbed surface species. In the former case, hysteresis occurs due to the potential drop across the Helmholtz layer resulted from the trapped holes at the surface states, and the magnitude of hysteresis, ΔE_F, is given by

$$\Delta E_F = e_0 \Delta N_{SS}/C_H \qquad (3)$$

where ΔN_{SS} is the change of the trapped hole density between the positive-to-negative sweep and the reverse sweep. By taking ΔE_F observed in sweeping the potential between −0.9 and 1.0 V vs SCE as 360 mV and C_H as 20 μF cm^{-2},[34,35] ΔN_{SS} is estimated to be $\sim 5 \times 10^{13}$ cm^{-2}, much larger than those for conventional MIS devices. For the latter case, hysteresis can also arise either by the transformation or desorption of surface species caused by acceptance of holes by the species, and the Si work function changes due to the change in the surface dipole. Consequently, the Si band edges shift, causing hysteresis in the C–V curve. The ΔE_F in this case is given by

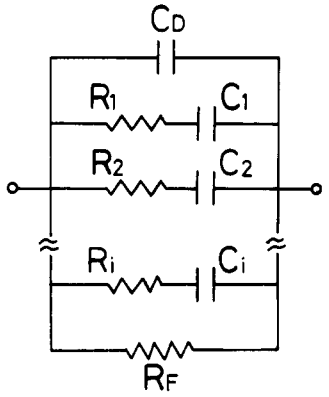

Figure 11. Equivalent circuit of Si electrodes immersed in electrolyte solutions, where C_i and R_i represent respectively the capacitance and resistance possibly due to surface states and an inversion layer, C_D is the depletion layer capacitance, and R_F is the faradaic resistance due to the majority carrier transport. Each parallel circuit possesses different time constants, $\tau_i = C_i R_i$.

$$\Delta E_F = \Delta \mu_S \Delta N_S/\epsilon_S \qquad (4)$$

where $\Delta \mu_S$ is the change in the normal component of the dipole moment of a surface species by accepting holes, ΔN_S is the change in the density of the surface species, and ϵ_S is the permittivity of the Si surface. If we take $\Delta \mu_S$ as 1 e_0 Å, for example, ΔN_S is calculated to be $\sim 2 \times 10^{14}$ cm^{-2}, ~20% of the surface Si density. By applying sufficiently negative potential, the surface species is reduced by electrons from the semiconductor, and the next sweep to the positive direction almost retraces the initial one. By expanding the potential sweep region more negative than −0.9 V, the C–V curve for the negative-to-positive sweep shows a cathodic shift due to the reduction of the surface species by electrons. Similar hysteresis is observed for InP electrodes immersed in an acetonitrile solution.[36,37]

The Peak in C–V Curves. The peaks observed in the C–V curves are usually attributed to surface states.[4,21-24] Lewis et al.[25] and we[26] have recently obtained the photovoltages of 670 and 695 mV, respectively, from the n-Si/methanol junction PEC cells. Such high photovoltages are possible only when the density of the surface recombination current is very low. Our recent analysis of the ideality factor[27] also indicates that the surface recombination rate is negligibly small. These results are incompatible with the assumption that the observed capacitance and conductance peaks are caused by the surface states. Instead, we propose an explanation that the peak is caused by minority carriers in the inversion layer, by the reasons explained below.

Figure 11 shows the equivalent circuit of the Si electrodes immersed in the electrolyte solution. C_D is the capacitance of the depletion layer, and the response time of the circuit is very short. Thus, the resistance in series to C_D is very small and ignored here. C_1 and C_2, etc., are the capacitances possibly due to surface states and to an inversion layer, and R_1 and R_2, etc., are the corresponding resistances. R_F is the faradaic resistance due to the majority carrier transport. The Helmholtz layer capacitance,

(34) Hansen, R. S.; Kelsh, D. J.; Gratham, D. H. *J. Phys. Chem.* **1963**, *67*, 2316.
(35) Breiter, M.; Delahay, P. *J. Am. Chem. Soc.* **1959**, *81*, 2938.
(36) Koval, C. A.; Austermann, R. L.; Turner, J. A.; Parkinson, B. A. *J. Electrochem. Soc.* **1985**, *132*, 613.
(37) Koval, C. A.; Austermann, R. L. *J. Electrochem. Soc.* **1985**, *132*, 2656.

which is in the range of about 20 μF,[34,35] is ignored since it is much larger than the capacitance measured in the present study. The admittance of the circuit, Y, is given by

$$Y = \frac{1}{R_F} + \omega^2 \sum \frac{C_i \tau_i}{1 + \omega^2 \tau_i^2} + j\omega \left(C_D + \sum \frac{C_i}{1 + \omega^2 \tau_i^2} \right) \quad (5)$$

where ω is the angular frequency and τ_i is the time constant, i.e., $\tau_i = C_i R_i$.

The background of the measured conductance shown by the dashed line in Figure 6 is due to R_F, and the peak is due to the second term in eq 5. Although the present system might contain various factors to influence the time response as discussed below, the time constant of the main element can be obtained from the plot of the conductance peak intensity, G_{peak}, divided by ω vs the frequency, since G_i/ω in eq 5 has the maximum value when $\omega\tau_i$ is equal to one. The plot of G_{peak}/ω measured in the dark shows a monotonic decrease with the frequency from 5 Hz as shown in Figure 7, and hence, the time constant is longer than 3×10^{-2} s. The time constant for surface states is usually in the range of 10^{-4} s,[16] much shorter than the obtained value. On the other hand, the inversion layer time constant is much longer in the dark since the minority carrier generation rate in the Si is very slow, in agreement with the experimental result.

The G_{peak}/ω measured under illumination has the maximum value at 1 kHz (Figure 7), and the corresponding time constant is estimated to be $\sim 2 \times 10^{-4}$ s. This reduction of the time constant by illumination can be explained by assuming that the conductance peak is due to minority carriers. Namely, the enhanced minority carrier density in the surface region can respond to a higher ac frequency. On the contrary, the time constant of surface states is expected to be hardly changed by illumination. This is because, under illumination, the minority carrier transport from the semiconductor to the surface states responds well to the ac signal owing to an increase in the minority carrier density. This transport occurs during the half cycle of the ac signal which moves the valence band toward the Fermi level, but, during the other half cycle, the transition of majority carriers from the semiconductor to the surface states is necessary to occur. Therefore, the total time constant is determined by the majority carrier time constant[16] even under illumination. The majority carrier time constant is unchanged by illumination since an increase in the majority carrier density is negligibly small compared to the donor density unless the Si is nearly intrinsic.

The slow G_{peak}/ω change with the frequency as shown in Figure 7 is attributed to the presence of transitions with various time constants. The potential is thought to be fluctuated over the Si surface mainly because that the density of the charged surface species is not uniform. Thus, the density of minority carriers at the surface is fluctuated, leading to inversion layer time constants varying from one surface position to another. Another possible cause of the broad distribution of the G_{peak}/ω is the presence of the hole transport process between the semiconductor valence band and a small amount of impurities in the solution. The time constant of this process is different from that between the Si surface and the bulk. The CR circuit to express this hole transport process may be necessary to be included in the equivalent circuit.

The Mott–Schottky plot for the n-Si electrode immersed in methanol at 195 K is linear in the voltage range between −0.8 and 0.1 V (Figure 8), indicating that the measured capacitance contains only the depletion layer component due to ionized donors. As the temperature is raised, the density of the minority carrier increases, and the plot begins to deviate from the straight line due to the contribution of the minority carrier capacitance to the depletion layer capacitance.

The slope of the straight portion of the Mott–Schottky plot changes with temperature since the ionization probability of the dopant is temperature dependent. The dopant density is estimated to be 7×10^{16} cm^{-3} from the Si resistivity of 0.1 Ω cm, in good agreement with that obtained from the slope of the Mott–Schottky plot at 303 K. From this donor density, the ionization probability is estimated to be 97, 96, and 87% respectively at 303, 275, and 195 K, considering that the donor level is 45 mV below the bottom of the conduction band.[38] Thus, the theoretical ratio of the slope of the Mott–Schottky plots at 195, 275, and 303 K is 1:0.91:0.90, and the slopes of the plots have this ratio.

In the presence of a redox couple in the solution (Figure 9), the hole quasi-Fermi level coincides with the redox level in the small bias region,[26] since a small amount of the hole-transfer current at the interface is sufficient to keep the hole quasi-Fermi level at the redox level. In this case, the bias is absorbed by the change in the depletion layer width, and the linear Mott–Schottky plot is obtained in the small bias region as shown in Figure 9 although the barrier height is high (1.06 V), and thus the inversion layer is formed at zero bias. As the bias voltage is increased, the hole-transfer rate becomes saturated, and consequently the hole quasi-Fermi level separates from the redox level due to the change in the hole density in the surface region.[26] In this case, the inversion layer capacitance is changed, and the Mott–Schottky plot deviates from the straight line.

Conclusion

The flat-band potential of the Si electrode immersed in the acetonitrile and methanol solutions of $LiClO_4$ or $NaClO_4$ shows an anodic shift after the electrode potential sweeps. The shift is caused by the inclusion of cations of the electrolytes in the SiO_2 layer during the formation of this layer by the reaction of Si with residual water in the nonaqueous solutions. Due to the shift of the flat-band potential, the barrier height is increased for the case of p-Si. The present electrochemical method of introducing cations in the SiO_2 layer may be useful for enhancing the photovoltages of MIS or PEC solar cells.

Peaks are observed in the C–V and G–V curves for the Si electrode immersed in these solutions. From discussions on the time constants of the transition for the peaks, the peaks are more likely due to minority carriers in the surface region than surface states.

Registry No. Me_2Fc, 1291-47-0; Me_2Fc^+, 12276-63-0; Si, 7440-21-3; SiO_2, 7631-86-9; CH_3CN, 75-05-8; CH_3OH, 67-56-1; $LiClO_4$, 7791-03-9; $NaClO_4$, 7601-89-0; Li, 7439-93-2; Na, 7440-23-5.

(38) Sze, S. M.; Irvin, J. C. *Solid-State Electron.* **1968**, *11*, 599.